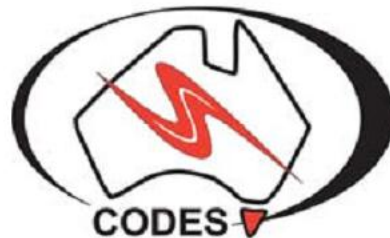


# **The petrogenesis and Ni-Cu-PGE potential of the Dido Batholith, north Queensland, Australia**

**Fiona C. Best**

BSc. (Hons.)

*A thesis submitted in fulfilment of the requirements for  
the degree of Doctor of Philosophy*



CODES ARC Centre of Excellence in Ore Deposits

University of Tasmania (UTAS), Australia

October 2012



## **Declaration of Originality**

This thesis contains no material which has been accepted for a degree or diploma by the University or any other institution, except by way of background information and duly acknowledged in the thesis, and to the best of the my knowledge and belief no material previously published or written by another person except where due acknowledgement is made in the text of the thesis, nor does the thesis contain any material that infringes copyright.

Signed

---

Fiona C. Best  
CODES, University of Tasmania  
October 2012

## **Authority of Access**

This thesis is not to be made available for loan or copying for two years following the date this statement was signed. Following that time the thesis may be made available for loan and limited copying and communication in accordance with the Copyright Act 1968.

Signed

---

Fiona C. Best  
CODES, University of Tasmania  
October 2012



Abstract

The Dido Batholith is a large north- to northeasterly-trending batholith, ~90 km long and up to 30 km wide, located along the southeastern margin of the Precambrian Georgetown Region (Greenvale Province), northern Queensland, Australia. It overlaps the contact between the Georgetown Region Precambrian rocks and the Early Palaeozoic volcano-sedimentary units of the northern end of the Tasman Fold Belt System. Hornblende-biotite tonalites and granodiorites are the dominant lithologies comprising this batholith, although an intermediate phase comprising hornblende-biotite diorites and gabbonorites dominates the southeastern quarter. Four elongate, km-scale, and several smaller mafic to ultramafic bodies (UMB) are hosted within this intermediate phase. All UMB are crosscut by abundant, texturally variable felsic to mafic dykes. New U-Pb zircon dates indicate that the diorite-gabbonorite phase crystallised at ~470 Ma, whereas the tonalite-granodiorite phase (named the Main Felsic Mass: MFM), UMB and associated mafic dykes crystallised at ~430 Ma. These new dates have led to the informal renaming of the older dioritic-gabbonorite phase as the Phantom Diorite, whereas the 430 Ma phases remain a part of the Dido Suite.

The km-scale UMB, which form the focus of this study, are layered cumulate sequences which represent open-system intrusions emplaced at shallow- to mid-crustal levels (15 – 25 km). They are divided into two petrographically and geochemically distinct varieties: (1) the low-Fe UMB (3 intrusions), comprising dunites, wehrlites, troctolites and olivine gabbro which contain variable amounts of olivine ( $\text{Fo}_{85-72}$ ), clinopyroxene ( $\text{Mg\# } 0.87 - 0.73$ ), plagioclase ( $\text{An}_{92-72}$ ) and chromites; and (2) the high-Fe UMB (1 intrusion), comprising dunites, wehrlites and pyroxenites which lack chromites and contain abundant, early crystallising Fe-Ti oxides and hornblende and less primitive olivines ( $\text{Fo}_{78-72}$ ) and pyroxenes ( $\text{Mg\# } 0.87 - 0.73$ ) than the low-Fe UMB. The high-Fe UMB displays moderate  $^{87}\text{Sr}/^{86}\text{Sr}_{(430)}$  (0.705932 – 0.706231) and negative  $\epsilon\text{Nd}_{(430)}$  (-3.1 to -4.0), whereas the low-Fe UMB displays lower  $^{87}\text{Sr}/^{86}\text{Sr}_{(430)}$  (0.703836 – 0.705318) and more positive  $\epsilon\text{Nd}_{(430)}$  (-0.9 to +3.7) values.

Using the composition of cumulus minerals and mafic dykes, it is estimated that the parent magmas of the low-Fe UMB contained 8 – 10 wt.% of both MgO and  $\text{FeO}_t$ , whereas the high-Fe UMB parent magmas were more evolved, having higher  $\text{FeO}_t$  (12 – 16 wt.%) and lower MgO (6.2 – 8.2 wt.%), Ni and Cr contents. The primary magmas of both the high- and low-Fe UMB are interpreted as mantle-derived arc rift or back-arc tholeiites. Crustal contamination during ascent is suggested to be responsible for the LREE-enriched and Nb- and Ti-depleted nature of the UMB parent magmas. Two-component isotope mixing models suggest that the addition of variable amounts (<5% in the low-Fe UMB and 9-10% in the high-Fe UMB) of 2000 – 2500 Ma igneous crustal contaminant to tholeiitic melts derived from a slightly enriched mantle source can account for isotopic compositions of the UMB. Although both the high-Fe and low-Fe UMB are interpreted as initially evolving along the tholeiitic liquid line of descent (LLD), the ultimate differentiation trend recorded by the high-Fe UMB is more akin to calc-alkaline fractionation, leading to tonalitic compositions. The higher volumes and relatively late addition

## Abstract

---

of crustal contaminants to the high-Fe UMB magmas (i.e. after they had experienced strong Fe-enrichment) is suggested to have resulted in this apparent shift in LLD.

The 430 Ma Dido MFM is a medium-K calc-alkaline intrusion, with relatively low  $^{87}\text{Sr}/^{86}\text{Sr}_{(430)}$  (0.706746), negative  $\epsilon\text{Nd}_{(430)}$  (-4.8) and a  $T_{\text{DM}}$  age of ~1390 Ma. It shows fractionated REE profiles ( $[\text{La}/\text{Yb}]_{\text{CN}} = 9.0 - 10.3$ ) and contains magmatic zircons with negative  $\epsilon\text{Hf}_{(430)}$  values (-0.9 to -5.9). The MFM is interpreted to have originated from a fractionated, mantle-derived melt which assimilated ~12% of 2000 - 2500 Ma igneous protocrust during ascent.

It is difficult to establish the exact relationship between the different phases of the Dido Suite although it is thought likely that most of the differences in magmatic trends between the individual phases are attributable to the physical conditions of magmatic evolution in the crust, rather than differences in initial magma types as: (a) isotopic differences between the individual UMB and MFM can be explained by variations in the amount of crustal contaminants assimilated into a common, mantle-derived magma, and the timing of this assimilation; (b) fractionation of cumulates similar to those comprising the low-Fe UMB likely drove the residual tholeiitic magma to become more enriched in Fe and  $\text{H}_2\text{O}$ ; and (3) later crustal contamination of such an evolved, Fe-enriched magma, and fractionation of Fe-Ti oxide-rich cumulates to produce the high-Fe UMB, may have generated a calc-alkaline LLD, eventually producing magmas with MFM-like compositions and isotopic signatures akin to the high-Fe UMB. As the latter process would require large volumes of mafic magmas and produce large cumulate sequences not seen at the current exposure level, these processes are required to have occurred at deeper crustal levels.

The 470 Ma Phantom Diorite is a medium-K calc-alkaline intrusion. It is geochemically similar to the Dido high-Fe UMB, displaying relatively low  $^{87}\text{Sr}/^{86}\text{Sr}_{(470)}$  (0.705775 to 0.706100), negative  $\epsilon\text{Nd}_{(430)}$  (-3.0 to -4.3) and  $T_{\text{DM}}$  ages of 1333 - 1461 Ma, with fractionated REE profiles ( $[\text{La}/\text{Yb}]_{\text{CN}} = 6.1 - 10.4$ ) and containing magmatic zircons with negative  $\epsilon\text{Hf}_{(470)}$  values (-1.64 and -8.69). These similarities suggest that (1) the Phantom Diorite and Dido Suite originated from the mixing of geochemically similar mantle-derived and crustal components and (2) that there was little change in the tectonic setting, and composition of the lithosphere beneath the Greenvale Province between the Mid-Ordovician (470 Ma) and Silurian (430 Ma). The striking geochemical similarities between the Dido high-Fe UMB and Phantom Diorite suggest both underwent a similar degree of crustal contamination (~8 - 12%).

Geochemistry and mineral compositions suggest that the 470 Ma Phantom Diorite and 430 Ma Dido Suite originated in an arc-backarc setting. Furthermore, although no Proterozoic rocks outcrop east of the Dido Batholith (the approximate position of the Tasman Line), the identified involvement of Proterozoic crustal contaminants in the genesis of the Dido Suite supports the ascent of these magmas through the Georgetown Region Precambrian crust of the North Australian craton. This, in turn, indicates genesis in a continental margin (Andean- or Mexican-type) arc setting, probably in an arc that

was actively rifting, given the tholeiitic nature of the primary magmas of the Dido UMB (and possibly the Dido MFM and Phantom Diorite). This finding largely supports the presence of a west-dipping subduction zone beneath the Greenvale Province during the Ordovician and Silurian.

As most of the large Ni-Cu-Platinum-group element (PGE) deposits worldwide have formed where mantle-derived melts intersect or are focussed along large faults in continental rift zones or rifted continental margins, Anglo American plc identified the southeast margin of the Georgetown Region, and specifically the Dido UMB, as a target for magmatic Ni-Cu-PGE deposits. No mineralisation has been found associated with the UMB. Rocks comprising the low-Fe UMB contain <1000 ppm Cu and <40 ppb of both Pt and Pd, whereas the high-Fe UMB rocks have similar Cu concentrations to the former but are generally more PGE-enriched (containing up to 160 ppb of both Pt and Pd). Geochemical discriminators suggest that the magmas that formed the km-scale UMB were chalcophile element-depleted, having undergone a previous S-saturation event (i.e. significant sulphide-deposition) at depth. Furthermore, based on their lower Cu/Zr ratios and highly Ni-depleted composition, the high-Fe magmas are interpreted to have experienced greater chalcophile metal loss than the low-Fe magmas. The PGE-enrichment in the high-Fe cumulates is therefore explained by the addition of PGE to the high-Fe magmas from an external source. Many economic Ni-Cu-PGE intrusions are interpreted as being formed from (a) the addition of batches of PGE-enriched magmas to resident, chalcophile element-depleted magmas (e.g. the Maracás deposit); or (b) scavenged PGE-rich sulphides which were carried to accessible crustal levels by later injections of magma (e.g. the Platreef). Either of these mechanisms could potentially account for the minor PGE-enrichment in the high-Fe UMB.

Although there is no evidence to suggest that large volumes of PGE-enriched sulphides were added to the Dido UMB magmas, considering the minimal exploration completed to date and the new PGE data suggesting the likely presence of significant volumes of PGE-rich sulphides at depth in this magmatic system, the UMB cannot be ruled out as potential targets for Ni-Cu-PGE deposits. Furthermore, although convergent settings rarely host economic Ni-Cu-PGE mineralisation, important exceptions such as the Aguablanca deposit (Spain), indicate that feeders or conduits to intrusions emplaced in local extensional regimes within subduction-related environments can generate important Ni-Cu sulphide deposits. Small mafic intrusions in convergent margin settings, particularly where local extension regimes are evident, should therefore not be overlooked in exploration for new Ni-Cu sulphide deposits and the remaining unexplored Dido UMB, including the high-Fe varieties and any other contemporaneous mafic-ultramafic intrusions in the surrounding area, should be evaluated on a case by case basis.





**Acknowledgements**

First and foremost, my deepest thanks go to my supervisor Tony Crawford for getting me involved in this project and for the constant guidance, encouragement, and advice throughout. I am incredibly grateful and have many fond memories. Thank you also to my secondary supervisor, Reid Keays, who provided much technical advice on the Ni-Cu-PGE investigations. Jeff Foster, Paul Davidson and Dave Hutchinson are also thanked for providing additional guidance.

I am also incredibly grateful to Anglo American Exploration Australia for their generous financial and logistical support and for allowing me the pleasure of being involved in such a great project. Particular thanks go to Paul Polito and Allan Kneeshaw.

My analytical work at the University of Tasmania was made possible by the assistance of several people: Sebastian Meffre who provided considerable help with the geochronological analysis and data reduction; Sarah Gilbert and Ian Little for help using the LA-ICPMS; and Karsten Goemann and Sandrin Feig for assistance with the Electron Microprobe (Central Science Laboratory). I am also grateful to Mark Fanning, Marc Norman and Emma Mathews at the Australian National University for assistance with the SHRIMP facility; Roland Maas at the University of Melbourne for preparation and analysis of Sr-Nd isotope samples; Jon Woodhead at the University of Melbourne for the analysis of zircon Hf-isotope samples; and Richard Friedman from the University of British Columbia for preparation and analysis of the sphene U-Pb sample.

I will never be able to express in words just quite how grateful I am to all my friends and family so here are just a few, rather understated, thanks. Firstly, thank you to my family - you have never discouraged me from following my dreams regardless of where they took me, and I will always be truly grateful for your altruistic and unfaltering support. Special thanks go to Andrew – having you here over the last year has been an absolute blessing and I'm a very lucky sister. Thank you to a long standing and very special friend, Catherine – you have always been an inspiration and I owe you for so many things. Also, thank you to Vicky – you have also been an inspiration and I am grateful for all your support and encouragement. Heartfelt thanks also go to those amazing friends who have become my Australian family – Jacqui, Emily, Adam, Gisela, Nat, Wen, Ben, Kate, Isa, Terrie. An extended shout out goes to Jacqui – thank you for your tireless moral support and encouragement, thank you for all the fun times and memorable adventures, thank you for letting me be a part of your lovely family and, well, thank you for being a great friend.

Last, but by no means least, a huge thank you goes to Paul - your love, support, patience and encouragement over the last year not only got me to my final destination but made the journey so much happier.



Contents page

<b>1</b>	<b>INTRODUCTION.....</b>	<b>1</b>
1.1	PREAMBLE .....	1
1.2	DETAILED AIMS AND OBJECTIVES.....	2
1.3	LOCATION AND ACCESS.....	3
1.4	EXPLORATION HISTORY.....	3
1.5	PREVIOUS WORK .....	4
1.6	WORKPLAN .....	5
1.6.1	<i>Fieldwork</i> .....	5
1.6.2	<i>Laboratory studies</i> .....	5
1.7	THESIS ORGANISATION AND FORMAT .....	6
<b>2</b>	<b>REGIONAL GEOLOGY.....</b>	<b>9</b>
2.1	OVERVIEW .....	9
2.2	PALAEOZOIC GREENVALE PROVINCE .....	12
2.2.1	<i>Regional setting</i> .....	12
2.2.2	<i>Geology</i> .....	12
2.2.3	<i>Deformation</i> .....	15
2.2.3.1	Structural characteristics .....	15
2.2.3.1.1	Foliation.....	15
2.2.3.1.2	Faults and mylonite zones.....	18
2.2.3.2	Timing of deformation .....	20
2.3	DIDO BATHOLITH.....	21
2.3.1	<i>Introduction</i> .....	21
2.3.2	<i>Geochronology</i> .....	21
2.3.3	<i>Geology</i> .....	22
2.3.4	<i>Deformation</i> .....	22
2.4	CRUSTAL FORMATION AND DEVELOPMENT IN THE GEORGETOWN REGION .....	23
2.5	GEODYNAMIC EVOLUTION OF THE GEORGETOWN REGION DURING THE LATE NEOPROTEROZOIC AND EARLY PALAEOZOIC .....	25
2.5.1	<i>Late Neoproterozoic - Early Cambrian</i> .....	25
2.5.2	<i>Cambrian - Ordovician</i> .....	25
2.5.3	<i>Silurian</i> .....	26
2.6	SUMMARY .....	28
<b>3</b>	<b>GEOLOGY OF THE DIDO BATHOLITH.....</b>	<b>29</b>
3.1	INTRODUCTION.....	29
3.2	GEOLOGY OF THE DIDO BATHOLITH .....	30
3.3	UMB.....	32
3.3.1	<i>Palmer Rails northerly UMB</i> .....	32
3.3.2	<i>Palmer Rails southerly UMB</i> .....	36
3.3.3	<i>Phantom northerly UMB</i> .....	39
3.3.4	<i>Phantom southerly UMB</i> .....	39
3.3.5	<i>Smaller UMB</i> .....	43
3.4	SUMMARY .....	43
<b>4</b>	<b>PETROGRAPHY.....</b>	<b>45</b>
4.1	MFM.....	45
4.2	MIM .....	45
4.2.1	<i>Diorites</i> .....	45
4.2.2	<i>Gabbronorites</i> .....	47
4.3	UMB.....	47
4.3.1	<i>Palmer Rails northerly</i> .....	47
4.3.1.1	Dunites .....	47
4.3.1.2	Wehrlites .....	48
4.3.1.3	Pyroxenites.....	48
4.3.1.4	Troctolite.....	51
4.3.1.5	Olivine gabbros/ gabbronorites .....	52
4.3.1.6	Olivine-free gabbros/ gabbronorites.....	54

4.3.2	<i>Phantom</i> .....	54
4.3.2.1	Troctolites .....	54
4.3.2.2	Olivine gabbros/ gabbronorites.....	55
4.3.2.3	Olivine-free gabbros/ gabbronorites.....	57
4.3.2.4	Marginal pegmatitic hornblende gabbros.....	57
4.3.3	<i>Palmer Rails southerly</i> .....	57
4.3.3.1	Dunites.....	57
4.3.3.2	Wehrlites.....	59
4.3.3.3	Olivine pyroxenites.....	59
4.3.3.4	Pyroxenites and hornblende pyroxenites.....	59
4.3.3.5	Melagabbros/ gabbronorites.....	63
4.3.3.6	Cumulate gabbros/ gabbronorites .....	63
4.4	DYKES.....	64
4.4.1	<i>Felsic dykes</i> .....	64
4.4.1.1	Garnet-bearing granites.....	64
4.4.1.2	Granodiorites, granites and tonalites.....	64
4.4.2	<i>Fine-grained intermediate – mafic dykes</i> .....	65
4.4.2.1	Diorites- gabbros.....	65
4.4.2.2	Dolerites.....	65
4.4.2.3	Monzogabbros .....	67
4.4.3	<i>Medium-grained mafic dykes</i> .....	67
4.4.4	<i>Pegmatitic mafic dykes</i> .....	67
4.5	SUMMARY .....	68
<b>5</b>	<b>GEOCHRONOLOGY</b> .....	<b>69</b>
5.1	INTRODUCTION.....	69
5.2	METHODOLOGY .....	69
5.2.1	<i>Zircon U-Pb geochronology</i> .....	69
5.2.1.1	Sample selection .....	69
5.2.1.2	Sample preparation & imaging .....	70
5.2.1.3	U-Pb isotopic analysis.....	71
5.2.1.3.1	SHRIMP analysis .....	71
5.2.1.3.2	LA-ICPMS analysis .....	71
5.2.2	<i>Sphene U-Pb dating: ID-TIMS</i> .....	72
5.2.2.1	Sample preparation .....	72
5.2.2.2	U-Pb isotope analysis.....	73
5.2.3	<i>Zircon Hf isotope analysis</i> .....	73
5.3	SAMPLE DESCRIPTIONS.....	74
5.4	RESULTS .....	74
5.4.1	<i>Zircon and sphene morphology</i> .....	74
5.4.2	<i>U-Pb isotope composition</i> .....	78
5.4.2.1	AUR100258: MFM tonalite.....	80
5.4.2.2	AUR100390: MIM diorite .....	82
5.4.2.3	AUR100406: MIM gabbronorite .....	84
5.4.2.4	AUR100605: MIM gabbronorite .....	84
5.4.2.5	AUR100303 and AUR100399: UMB marginal pegmatitic hornblende gabbros .....	84
5.4.2.6	AUR100564: Hornblende gabbro dyke.....	85
5.4.2.7	AUR100606: Hornblende gabbro dyke.....	85
5.4.3	<i>Lu-Hf zircon isotope compositions</i> .....	87
5.5	DISCUSSION AND SUMMARY.....	87
5.5.1	<i>'Dido Suite' crystallisation ages</i> .....	87
5.5.2	<i>Dido Suite and Phantom Diorite magma sources and assimilation</i> .....	89
5.5.3	<i>Comparison of Hf-isotope data to other Georgetown Region Pama Province granites</i> .....	91
5.5.4	<i>Implications for the Georgetown Region</i> .....	92
<b>6</b>	<b>DIDO SUITE - MINERAL CHEMISTRY</b> .....	<b>95</b>
6.1	INTRODUCTION.....	95
6.2	METHOD .....	95
6.3	MINERAL COMPOSITIONS .....	97
6.3.1	<i>Olivine</i> .....	97
6.3.2	<i>Oxides</i> .....	104
6.3.2.1	Chrome-spinel and chrome-magnetite: Low-Fe UMB.....	104
6.3.2.2	Magnetite .....	111
6.3.2.2.1	High-Fe UMB .....	111
6.3.2.2.2	Low-Fe UMB .....	116
6.3.2.2.3	MFM .....	117

6.3.2.2.4	Dykes.....	117
6.3.2.3	Ilmenite.....	117
6.3.3	<i>Clinopyroxene</i> .....	121
6.3.4	<i>Orthopyroxene</i> .....	126
6.3.5	<i>Plagioclase</i> .....	128
6.3.6	<i>Amphiboles</i> .....	134
6.4	CUMULATE MINERAL PROFILES.....	138
6.5	MINERAL THERMOMETERS AND BAROMETERS.....	138
6.5.1	<i>Two-pyroxene thermometers and barometers</i> .....	138
6.5.2	<i>Al-in-hornblende thermobarometer</i> .....	141
6.5.3	<i>Magnetite-ilmenite pairs</i> .....	142
6.6	DISCUSSION.....	144
6.6.1	<i>Post-cumulus chemical modification</i> .....	144
6.6.1.1	Olivines.....	144
6.6.1.2	Spinel.....	147
6.6.1.3	Fe-Ti oxides.....	149
6.6.1.4	Pyroxenes.....	152
6.6.1.5	Plagioclases.....	153
6.6.1.6	Amphiboles.....	153
6.6.1.7	Coronas.....	153
6.6.2	<i>Petrogenetic implications</i> .....	154
6.6.2.1	Origin of the Fe-Ti oxides: High-Fe UMB.....	154
6.6.2.2	Composition and nature of the primitive melts of the UMB.....	158
6.6.2.3	Magma chamber processes: UMB.....	160
6.6.2.3.1	In situ crystallisation?.....	160
6.6.2.3.2	Open vs. closed systems.....	160
6.6.2.3.3	Crystallisation sequence.....	161
6.6.2.3.4	Sulphide saturation.....	162
6.6.2.3.5	Melt removal.....	163
6.6.2.4	Pressure conditions during emplacement.....	164
6.6.3	<i>Implications for tectonic setting</i> .....	165
6.6.3.1	Olivines.....	166
6.6.3.2	Spinel.....	166
6.6.3.3	Pyroxenes.....	169
6.6.3.4	Plagioclase.....	170
6.6.3.5	Amphiboles.....	172
6.7	SUMMARY.....	173
<b>7</b>	<b>DIDO SUITE – GEOCHEMISTRY.....</b>	<b>175</b>
7.1	INTRODUCTION.....	175
7.1.1	<i>Previous work</i> .....	175
7.1.2	<i>Aims and objectives</i> .....	176
7.2	METHODS.....	177
7.3	RESULTS.....	177
7.3.1	<i>Major elements</i> .....	177
7.3.2	<i>Trace elements</i> .....	188
7.3.3	<i>REE</i> .....	190
7.3.4	<i>Incompatible elements</i> .....	196
7.3.5	<i>Sr-Nd isotopes</i> .....	199
7.3.5.1	Initial $^{87}\text{Sr}/^{86}\text{Sr}$ and $\epsilon\text{Nd}$ .....	199
7.3.5.2	Depleted mantle model ages.....	205
7.4	DISCUSSION.....	206
7.4.1	<i>Composition and nature of the primitive melt of the UMB</i> .....	206
7.4.1.1	Low-Fe UMB.....	208
7.4.1.2	High-Fe UMB.....	212
7.4.2	<i>Two component mixing models</i> .....	215
7.4.2.1	Modelling with trace element data.....	215
7.4.2.2	Modelling with Sr-Nd isotopic data.....	216
7.4.2.2.1	Mantle-derived component (MC).....	217
7.4.2.2.2	Crustal-derived component (CC).....	217
7.4.2.2.3	Mixing of CC and MC.....	219
7.4.3	<i>Petrogenesis of the Dido Suite</i> .....	221
7.4.3.1	Low-Fe UMB.....	221
7.4.3.2	High-Fe UMB.....	222
7.4.3.3	MFM.....	223
7.4.3.4	Relationships between the Dido Suite UMB and MFM.....	223

## Contents page

7.4.4	<i>Relationship between the Dido Suite and other Pama Province granites in the Georgetown Region</i>	224
7.4.5	<i>Tectonic setting of intrusion of the Dido Batholith</i>	225
7.5	SUMMARY	225
<b>8</b>	<b>DIDO UMB – PGE GEOCHEMISTRY AND MINERALISATION POTENTIAL</b>	<b>227</b>
8.1	INTRODUCTION	227
8.2	METHODS	227
8.3	RESULTS	227
8.3.1	<i>Platinum, Pd and Au concentrations</i>	227
8.3.2	<i>Iridium and Rh concentrations</i>	229
8.3.3	<i>Mantle-normalised PGE profiles</i>	229
8.3.4	<i>UMB: chemical variations across stratigraphy with respect to PGE</i>	231
8.3.5	<i>Se and S/Se ratios</i>	233
8.4	DISCUSSION	234
8.4.1	<i>Variations and controls of Ni, Cu and PGE in the Dido UMB</i>	234
8.4.2	<i>PGE geochemistry: Implications for the petrogenesis of the Dido UMB</i>	236
8.4.3	<i>S/Se: Assessing crustal contamination</i>	236
8.4.4	<i>Ni-Cu-PGE fertility of the UMB magmas</i>	237
8.4.5	<i>Tectonic setting of emplacement: implications for exploration</i>	239
8.4.6	<i>Comparing the Dido UMB to other mineralised intrusions</i>	240
8.5	SUMMARY OF THE NI-CU-PGE POTENTIAL OF THE DIDO UMB AND SURROUNDING AREA	243
<b>9</b>	<b>PHANTOM DIORITE - MINERAL CHEMISTRY AND GEOCHEMISTRY</b>	<b>245</b>
9.1	INTRODUCTION	245
9.2	METHODS	245
9.3	RESULTS	246
9.3.1	<i>Mineral chemistry</i>	246
9.3.1.1	<i>Clinopyroxene</i>	246
9.3.1.2	<i>Orthopyroxene</i>	247
9.3.1.3	<i>Plagioclase</i>	247
9.3.1.4	<i>Amphiboles</i>	251
9.3.2	<i>Mineral barometry</i>	252
9.3.3	<i>Geochemistry</i>	253
9.3.3.1	<i>Major elements</i>	253
9.3.3.2	<i>Trace elements</i>	256
9.3.3.3	<i>REE</i>	257
9.3.3.4	<i>Incompatible elements</i>	259
9.3.3.5	<i>Sr-Nd isotopes</i>	260
9.4	DISCUSSION	262
9.4.1	<i>The origin and evolution of the Phantom Diorite</i>	262
9.4.2	<i>Comparing the origins of the 470 Ma Phantom Diorite and 430 Ma Dido Suite</i>	263
9.5	SUMMARY	264
<b>10</b>	<b>CONCLUSIONS</b>	<b>265</b>
	<b>REFERENCES</b>	<b>269</b>

**Appendices**

- Appendix 1:** Electron microprobe analyses of olivine, Cr-spinel, ilmenite, Fe-Ti oxides, clinopyroxene, orthopyroxene, plagioclase and hornblende from the Dido Suite and Phantom Diorite
- Appendix 2:** Details of the methods used to gain whole rock major and trace element data
- Appendix 3:** Whole rock major and trace element data for all analysed samples from the Dido Suite and Phantom Diorite
- Appendix 4:** LA-ICPMS analyses of clinopyroxene, plagioclase and olivine from selected samples from the Dido UMB